A Comparison Among Different Methods to Estimate Vehicle Sideslip Angle

Flavio Farroni, Nicola Pasquino, Ernesto Rocca, Francesco Timpone

Abstract—Accurate measurement of the vehicle sideslip angle is fundamental to improve reliability of the vehicle dynamics control systems focused on stability and developed both for safety and performance optimization. Many experimental procedures to estimate the vehicle sideslip angle have been proposed in the last years, mainly based on GPS, INS and physical models.

The aim of this paper is to compare different methods to estimate sideslip angle employing an instrumented vehicle, equipped with a system for data acquisition and time-synchronized storage capabilities, a stand-alone GPS, a GPS aided MEMS-based Attitude and Heading Reference System (AHRS) and specific sensors to collect data on the steering wheel angle and on the position of brake, throttle and clutch pedals. Further information is collected by capturing the available data at the OBD port of the vehicle. Data acquisitions (from all sensors) are synchronized by means of an external triggering signal.

After driving sessions performed with specific manoeuvres in order to highlight the main phenomena concerned with the dynamic behaviour of the vehicle, the different estimation procedures have been applied, discussing on the advantages and the degree of reliability of each one of them.

Index Terms— Differential GPS Tracking, Inertial Navigation System, Instrumented Vehicle, Physical Modelling, Vehicle Sideslip Angle.

I. INTRODUCTION

REAL-TIME knowledge of the vehicle sideslip angle (β) (the angle the vehicle center of gravity velocity (V_G) forms with the longitudinal vehicle axis (x)) is a fundamental issue to manage all vehicle's control systems [1] such as braking [2]-[24], stability [5] and many ADAS control systems [6], as well as a very important factor allowing to validate driving simulators [7], [8].

In the event of low-friction situations, it is advantageous to control the vehicle sideslip angle, preventing it from assuming unexpected values [9], [10]. However, despite the absolute benefits deriving from the direct measurement of

Manuscript received March 20, 2015.

Flavio Farroni is with Dipartimento di Ingegneria Industriale, Università degli Studi di Napoli Federico II, via Claudio n. 21 80125 Napoli Italy (e-mail: flavio.farroni@unina.it).

Ernesto Rocca is with Dipartimento di Ingegneria Industriale, Università degli Studi di Napoli Federico II, via Claudio n. 21 80125 Napoli Italy (e-mail: ernesto.rocca@unina.it).

Francesco Timpone is with Dipartimento di Ingegneria Industriale, Università degli Studi di Napoli Federico II, via Claudio n. 21 80125 Napoli Italy (corresponding author: phone: +39 081 76 83263; fax: +39 081 2394165; e-mail: francesco.timpone@unina.it).

Nicola Pasquino is with Dipartimento di Ingegneria Elettrica e delle Tecnologie dell'Informazione, Università degli Studi di Napoli Federico II, via Claudio n. 21 80125 Napoli Italy (e-mail: nicola.pasquino@unina.it).
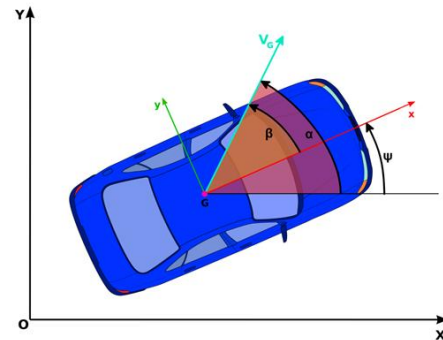
Fig. 1. Vehicle Dynamics characteristic Angles.

the sideslip angle and absolute vehicle velocity, these values are not usually directly measured on production cars and therefore must be estimated [11], [12].

While the yaw rate (r=dψ/dt) can be easily measured by a gyroscope, Fig. 1 shows that the estimation of the vehicle sideslip angle requires the knowledge of the vehicle heading (ψ) and of the direction of the center of gravity's velocity vector (α) (all of them expressed with respect to a dedicated reference system).

Because of the fundamental importance of β for vehicle dynamics, several methods have been developed over the years for its estimation. All the different existing methods display some strong points, but even some weaknesses, so that a universally valid and advantageous method has not been developed yet.

The most widely adopted methods are briefly described in the following, together with their main advantages and disadvantages, as well as their main fields of application.

A. Single Antenna GPS

The magnitude and the direction of the center of gravity velocity vector (V_G) can be easily determined once a suitable reference system has been identified thanks to a GPS receiver.

Depending on the specific receiver in use, the information about the velocity vector can be obtained directly (some models are able to provide the velocity vector's components expressed in the reference system the device has been referred to) or has to be determined in an indirect way. The latter is the case of a GPS receiver only indicating the sequence of the taken position at any single time. In this case, by simple kinematic considerations, being the elapsed time between two consecutive points known, also the velocity vector's magnitude can be determined.

Once the velocity vector pertaining to the vehicle's center of gravity has been fully characterized in its components, the α angle is defined with respect to the assumed coordinate system. If the vehicle is equipped with some

gyroscopes, then their signal can be integrated, and the vehicle's heading angle (ψ) can be obtained. From the knowledge of these two angles, the vehicle sideslip angle β is immediately determined.

One of the main limits affecting this procedure is represented by its variable accuracy: position uncertainty in a modern GPS is largely determined by the number of satellites in view and can reach in some cases the unacceptable magnitude of a few meters.

For these reasons, the single-antenna-GPS method is often integrated with some correction algorithm, such as the differential correction method [13]. Other improvements of this method use a higher number of GPS like the Double Antenna GPS method discussed below.

B. Double Antenna GPS

Also a double antenna GPS can be used for vehicle sideslip angle measurement [12], [14]: either two separate GPS receivers or a single receiver equipped with two different antennas can be used, theoretically obtaining equivalent accuracy. The purpose of using two different antennas is to directly calculate the vehicle's orientation with respect to an 'absolute' reference coordinate frame, with no necessity of using an additional gyroscope.

Using a double-antenna GPS two different points of the same vehicle, which can be assumed as a completely rigid body, can be simultaneously characterized.

The use of a double-antenna GPS is very easy to understand since a single-antenna GPS cannot measure the vehicle sideslip angle by itself, but always needs to be flanked by a gyroscope.

C. Inertial Navigation System signals Direct Integration Procedures

One of the easiest ways to determine the vehicle sideslip angle consists in the direct integration of the signals coming from the accelerometers and gyroscopes (or, more often, from the Inertial Navigation System (INS) based on the advanced application of inertial sensors (accelerometers) and rotational speed sensors (gyroscopes)) installed on-board the vehicle itself [15].

Thanks to this method, no vehicle model nor other instrument is needed. The results obtained from the adoption of this simple procedure are not always acceptable, because they tend to be affected by a high rate of error, since they are based on the direct integration of the accelerometer signals.

D. Physical models

This approach for the sideslip angle estimation is based on the use of some physical models, possibly running in real-time, describing the vehicle's behavior, such as the 'Bicycle model' or the 'Quadricycle model' [16].

Once the chosen physical model is known, in order to determine the vehicle sideslip angle, it is sufficient to strictly apply the model's equations.

The precision of the obtained results is highly affected by the degree of complexity of the employed model, that is by the reliability of the physical and geometrical parameters inserted in the model, like the vehicle's characteristic lengths and dimensions, its inertial features, transmission ratios, tyres' behavior parameters and so on [17].

II. EXPERIMENTAL EQUIPMENT

A. Vehicle

The experimental tests have been carried out on a FIAT Multipla 1.9 JTD, made available by the DICEA (Department of Civil, Architectural and Environmental Engineering) of University of Naples 'Federico II' [18]. This vehicle has been used extensively in past researches to monitor the behaviour of a driver both for analytical model formulation [19], and for testing of Driving Assistance Systems (DAS) logics.

In order to define the considered test-vehicle as precisely as possible, its physical and geometric parameters have been carefully evaluated by means of the available technical sheets.

Tyre behaviour has been modelled by means of a 'Magic Formula' model. The vehicle was equipped with the measurement instruments described in the following.

B. Description of the installed hardware

The vehicle is equipped with a system for data acquisition and time-synchronized storage capabilities. The core of the system is a National Instruments (NI) CompactDAQ chassis, with up to eight measurement-specific modules. All the sensors installed on-board are in direct communication with the DAQ's control software.

The DAQ receives digital and analog signals via appropriate modules, as well as data and communications via a CAN (Controlled Area Network) interface. In order to process the big amount of acquired data, the CompactDAQ is connected to a PC controller. The synchronization and acquisition software is based on LabVIEW.

A TOPCON GPS supplies positioning and kinematic data using a dual satellite constellation (GPS and GLONASS). The GPS is equipped with an external antenna, installed on the vehicle's rooftop. The GPS dual-frequency receiver is equipped with an internal memory allowing to store raw satellite data for post-processing applications. An XSENS MTi-G device embedding a GPS and an Inertial Measurement Unit (IMU), together with an AHRS processor have been placed on-board as near as possible to the center of gravity (G), with the aim of minimizing the centripetal acceleration deriving from the rotations of the vehicle. The GPS system complements the inertial system by providing a stable position and velocity output. As a result, the errors introduced by integrating accelerometer and gyroscope signals (dead reckoning) are corrected by the position and velocity given by the GPS receiver, resulting in an output that is both stable and able to track fast changing movements.

Three potentiometers are used to collect data on the position of the brake, throttle and clutch pedals. The steering wheel angle is measured by a draw-wire displacement sensor.

Other on-board information is also collected by capturing the available data at the OBD (On Board Diagnostic)-II port of the vehicle. Data acquisitions (from all sensors) are synchronized by means of an external triggering signal.

The MTi-G control logic is based on inertial sensors and a miniature GPS receiver, also including other supporting sensors, such as a 3D magnetometer and a static pressure transducer.

Orientation data are provided as relative orientation between the above-defined reference system and the LTP (Local Tangent Plane) reference system. LTP is a reference system defined by the tangent plane to the Earth surface in every point. According to the axes' orientation, it is possible to distinguish between different reference systems, such as LTP_{enu} ('East North Up') or LTP_{nwu} ('North West Up'). The 'default' LTP reference system with respect to which the XSENS provides the results is LTP_{nwu}.

III. DATA ACQUISITION AND PRE-PROCESSING

A. Available Data Channels

A LabVIEW script has been used for the acquisition of data from the different on-board instruments, with a sampling frequency of 10 Hz.

The collected GPS data are the time, the latitude, the longitude, and the altitude of the GPS antenna, hemispheres (North or South and East or West), the speed of the GPS antenna and the number of visible satellites.

The following data are gathered from the XSENS sensor: the three Euler angles (roll, pitch, and yaw components around vehicle longitudinal, lateral and vertical axes the three angular velocities of vehicle (roll, pitch, and yaw rate) and the three linear accelerations of vehicle (longitudinal, lateral, and vertical acceleration).

Data from the other sensors are the steering wheel angle (positive for clockwise rotation out of neutral position), the longitudinal speed of both the rear wheels of vehicle (computed by means of a rotational encoder), the normalized excursion of the vehicle pedals (brake, clutch, and throttle pedals), and the engine's rotation speed).

By direct connection to the XSENS device, some other useful information can be retrieved, the main one being the components of the vehicle's velocity vector in the LTP_{nwu} reference system.

IV. DRIVE SESSIONS

In this section a description of the performed tests is reported, together with a brief description of the particular 'test protocol' implemented.

A. Experimental Site

Some preliminary test drives have been performed close to the location of the Engineering Faculty of the University of Naples Federico II in order to become familiar with the measurement equipment, configure it.

The final test session has been carried out on a closed race track, an open-sky and abandoned parking area of a mall in Northern Naples (coordinates: 40.896776° N; 14.312782° E). The site fulfils the experimental requirements: no vehicle transit, no considerable obstructions to GPS signals, and quite planar area.

Some fixed elements in the site, such as road markings, are used to define the reference points of each manoeuvres performed in the test session.

Test drives were performed in dry road and good weather conditions (cloud-free sky).

B. Test Protocol Definition

The test protocol has been defined following the criterion of performing manoeuvres determining a considerable
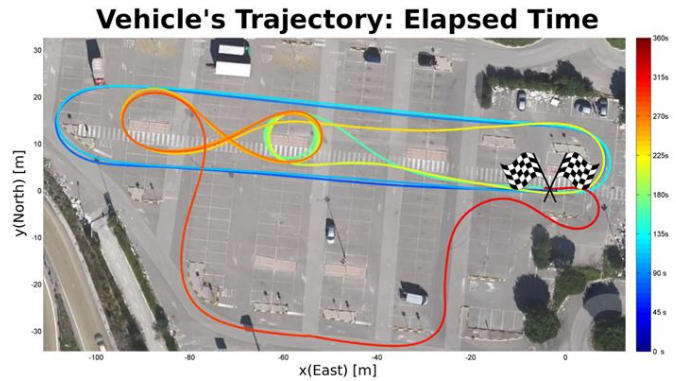

Fig. 2. Vehicle's trajectory during the performance of the defined test protocol, superimposed to the satellite image of the selected area, and colored according to the elapsed time from the beginning of the drive session [Blue=Initial position; Red=Final position]. The initial and final points coincide, and have been marked with the chess flags.

sideslip angle occurrence.

In the following the different steps of the chosen test protocol for the drive sessions are reported(Fig. 2):

Start: all the simulations start and finish at the same point, marked with the chess flags.

Idle Period: before any drive is performed, a preliminary acquisition with stationary vehicle has to be carried out, with the aim of identifying the bias affecting all the instrumental signals. The idle period usually lasts some tens of seconds.

Straight drive: all drive sessions start with a set of straight drives on a closed loop, separated by curves to revert the direction. The straight drive are used to validate the initial condition on yaw angle, computed by means of a compass: if the compass procedure is correct, during the straight drive the vehicle sideslip angle is supposed to be null, as the centre of gravity's velocity vector is perfectly aligned with the vehicle's heading.

Circle drive: performed with constant steering angle and constant vehicle speed to get a constant sufficiently high vehicle sideslip angle [20].

"8" shaped manoeuvres: after the circle drive some manoeuvres on a "8-shaped" trajectory have been performed. Also in this case, this manoeuvre has the purpose of letting some higher vehicle sideslip angles occur.

Hard Braking: the final path consists in a straight drive, with a very hard braking manoeuvre performed at sustained speed, aiming to determine tyres' lock up and subsequent ABS logic intervention.

Stop: the drive session stops in correspondence of the same point it started. Thanks to the white stripes on the road surface, the exact point can be found, and the vehicle's final orientation is made to be approximately coincident with the initial one.

The different phases of the above described test protocol can be easily discerned on the sample vehicle sideslip angle plot (obtained by means of 1Cbis differential GPS procedure explained in the following), traced against measurement time. The different steps of the data acquisition session can be discerned (Fig. 3); in particular:

Idle Period: this phase can be easily recognized in the plot, as the sideslip angle has been put null when the vehicle is not moving ($V_G < 5$ km/h).

Straight drive: as it is evident, during a straight drive the vehicle sideslip angle is equal to zero, since the direction of

the V_G vector is coincident with the direction of the vehicle-anchored x axis, indicating the vehicle's heading.

In Fig. 3 it is possible to see that the straight drive portions are characterized by null sideslip angle indeed: the visible regular spikes represent the cyclic curves performed to invert the vehicle's direction, as depicted in previous Fig. 2. All the spikes have the same sign, since all the curves have been performed in the same direction (clockwise).

Circle drive: as above described, the circle drive manoeuvre has been performed with constant steering angle and vehicle speed. This feature allows a very rapid identification of this particular drive session's step in the plot of the vehicle sideslip angle, as the β signals oscillates around a well-defined value, different from zero.

"8" shaped manoeuvres: this path can be discerned in the plot considering that during an "8" shaped manoeuvre curves are performed in both directions, so that the steering wheel has to pass through the 'neutral' position at every inversion. For this reason, it is easy to understand the vehicle sideslip angle oscillates around an approximately null value, reaching about the same magnitude in both directions, as depicted in Fig. 3.
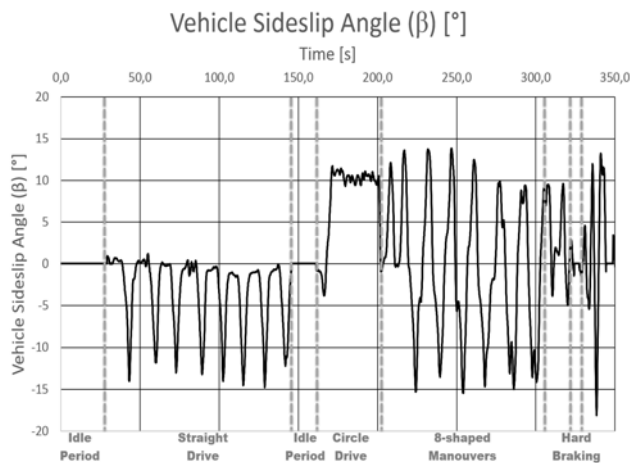

Fig. 3. Sample vehicle sideslip angle plot vs. measurement time.

Hard Braking: the hard braking can be easily discerned from the vehicle sideslip angle plot by the null portion of the curve, corresponding to the vehicle complete stop after the braking process.

The slight oscillation right before the null value (before the vehicle has come to a complete stop) is due to the fact the vehicle is rapidly decelerating, so that the lateral component of velocity is comparable with the longitudinal one, making sideslip angle value oscillating.

V. IMPLEMENTED PROCEDURES AND RESULTS

To estimate the vehicle sideslip angle different procedures have been employed based on GPS, on INS Signal Direct Integration and on Bicycle Model.

A. GPS

The first procedure (1A) makes use of the XSENS device, using both the GPS receiver and the gyroscopes.

The vehicle sideslip angle is determined as the difference between the α and ψ angles, computed with respect to the LTP_{enu} frame (Fig. 1).

The α angle is determined once the components of the center of gravity's velocity vector (V_G) are known, from the

XSENS data acquisition. It is important to underline that the XSENS platform automatically calculates the velocity vector's components in the LTP_{nwu} reference system.

As it is evident in Fig. 4, starting from the vector's component it is immediate to obtain the α angle as:

$$\alpha = \tan^{-1}\left(\frac{V_{North}}{V_{East}}\right) = \tan^{-1}\left(\frac{V_Y}{V_X}\right) \qquad (1)$$
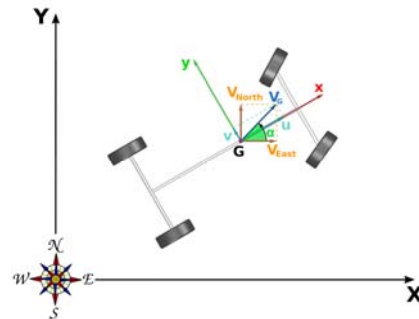

Fig. 4. Decomposition of the vehicle's centre of gravity's velocity vector along the moving vehicle-anchored $\{Gxyz\}$ reference system and along the absolute $\{PXYZ\}$ reference system.

The ψ angle can be obtained either directly from the XSENS platform or by the integration of the vehicle's yaw rate signal, acquired by the INS sensor.

Also the second procedure (1B) makes use of the XSENS device, using both the GPS receiver and the gyroscopes, and simply applies the vehicle sideslip angle definition, reporting the velocity vector's components into the moving, vehicle-anchored $\{Gxyz\}$ reference system to know the u and v components.

Once the u and v components have been determined, the vehicle sideslip angle is simply determined as:

$$\beta = \tan^{-1}\left(\frac{v}{u}\right) \qquad (2)$$

The third procedure (1C) makes use of both the TOPCON GPS and XSENS devices.

The vehicle sideslip angle is determined as in the previous procedure 1A, but in this case the α angle is obtained thanks to a different method.

The TOPCON GPS receiver simply provides the terrestrial coordinates of all the points belonging to the vehicle's trajectory (with a data rate depending on the configured working frequency), and the magnitude of the velocity vector needed to connect two consecutive points $P1$ and $P2$.

In order to compute the α angle, some simple kinematic consideration are employed (Fig. 5).

The instantaneous velocity of the vehicle in the $P1$ point can be obtained as:

$$V(t) = \lim_{\Delta t \to 0} \frac{\Delta s}{\Delta t} \qquad (3)$$

In such cases, the instantaneous velocity vector can be assumed to be parallel to the displacement vector at any given time, whose direction can be easily identified through the difference of the coordinates recorded by the GPS receiver. Once the velocity vector has been fully identified, its inclination angle α is used for the calculations.

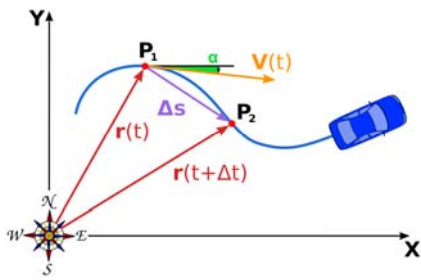Regarding the ψ angle, it can be obtained either directly

Fig. 5. Determination of the instantaneous vehicle's velocity vector starting from its centre of gravity's trajectory.

from the XSENS platform or integrating the vehicle's yaw rate signal acquired by the gyroscope.

One of the main limitations affecting the preciseness of the just described procedure is represented by its heavy dependence on the quality of the GPS signal, hence from the number of satellites in view of the receiver.

For this reason, some signal improvements have been performed in order to increase the accuracy of the sideslip angle estimation in the following procedure.

The fourth procedure (1C bis) is very similar to the 1C one, since it is based on the same physical and analytical considerations. The only difference between the two procedures is represented by the GPS data acquisition: in order to enhance the signal's preciseness and reliability a differential correction has been applied [13].

In the differential procedure (DGPS) a GPS receiver tracking a satellite always experiences a number of ranging errors, which will be translated into positioning errors. The commonality of range errors between two receivers simultaneously tracking a satellite at two different locations can be exploited: common errors can be removed by differencing. Recording simultaneous range observations allows differential processing at a later time, or in real time, if a suitable communication device is available.

The differential correction considered in the current paper has been carried out off-line, referring to the ephemeris data published online after the data acquisition session was performed.

A highly precise GPS device('Trimble' GPS: receiver and antenna) has been positioned in a fixed place for the differential procedure application and has been used as the reference station, in order to differentiate the data acquired by the TOPCON GPS (the mobile station).

In order to allow the reference station to fix its position, the reference GPS has been placed in position about 1 hour before the drive sessions' beginning.

B. INS Signal Direct Integration

These procedures only use the accelerometers' signal, obtained from the XSENS acquisition.

The first procedure (2A) is a purely kinematic method for the vehicle sideslip angle determination, based on the integration of the accelerometers' signals; for this reason, the only required instruments are the accelerometers and the gyroscopes.

The accelerometers provide a measurement of acceleration referred to the vehicle-anchored moving reference system $\{Gxyz\}$. To express the center of gravity's acceleration vector a_G with respect to the LTP$_{enu}$ reference system it is necessary to implement a coordinate

transformation, so all the calculations are performed in the absolute reference system. A crucial importance is assumed by the Euler Angles used since these highly affect the obtained accelerations in the $\{Gxyz\}$ reference system, and in turn the resulting velocities and sideslip angle [21].

By integration of the acceleration components the velocities, expressed in the 'absolute' LTP$_{enu}$ reference system, are obtained.

The initial condition for the integration of the accelerations has been set to zero as the vehicle had null velocity during the first acquired seconds (idle period).

After integration, the velocity components have to be reported again into the $\{Gxyz\}$ moving reference system. At this point, the u and v components, namely the V$_G$ components in the $\{Gxyz\}$ reference frame, have been obtained, hence it is immediate to obtain the desired vehicle sideslip angle as (2).

The second Procedure (2B) calculates the vehicle sideslip angle making use of the XSENS inertial station and of the rotational encoder fitted on the rear wheels.

This procedure is based on the vehicle sideslip angle definition, (2).

Regarding the u component, this has been directly measured through the rotational encoders installed on the vehicle's rear wheels (it is calculated as the mathematical average of the values provided by the two encoders).

The v component has been obtained from the Equation reported below, where the lateral component of the a_G vector with respect to the $\{Gxyz\}$ vehicle-anchored moving reference system is defined:

$$a_y = \dot{v} + u \cdot r \quad \Rightarrow \quad \dot{v} = a_y - u \cdot r \qquad (4)$$

Where the yaw rate r is measured by the gyroscope.

Once the u and v components have been obtained, the vehicle sideslip angle is obtained by applying its definition.

The third procedure (2C) aims to determine the vehicle sideslip angle starting from the signals obtained from the accelerometers and gyroscopes embedded into the XSENS inertial station, installed on-board.

This procedure makes use of the following Equations:

$$\begin{cases} a_x = \dot{u} - v \cdot r \\ a_y = \dot{v} + u \cdot r \end{cases} \Rightarrow \begin{cases} \dot{u} = a_x + v \cdot r \\ \dot{v} = a_y - u \cdot r \end{cases} \qquad (5)$$

Once the a$_x$, a$_y$ and $r = $ dψ/dt quantities have been obtained from the XSENS data, these equations can be solved, determining the u and v.

Once the u and v components have been obtained, the vehicle sideslip angle is obtained by applying its definition.

C. Bicycle Model

This procedure uses a vehicle dynamics' physical model to predict the vehicle sideslip angle, given the input parameters.

The physical model considered for the current paper is the so-called bicycle model [16].

Both the kinematic bicycle model (absence of drift) and the dynamic bicycle model (with drift) have been considered, in order to provide a comparison between the different cases.

In the first procedure (3A) the Classic Kinematic Bicycle

is used, which is only valid in case of low vehicle's speed and high curvature radius of the performed trajectory, and therefore very uncommon to be observed in actual conditions. The input signals for this model are the vehicle's longitudinal speed (u) and the steering angle of the vehicle's front wheels (δ).

The vehicle sideslip angle, in case of kinematic conditions, can be easily determined by means of simple geometric and trigonometric considerations, Fig. 6. Being the (ACB)ˆangle equal to δ, it is immediate to obtain:

$$\beta = \tan^{-1}\left(\frac{a_2}{R}\right) \quad \delta = \tan^{-1}\left(\frac{l}{R}\right) \quad R = \frac{l}{\tan\delta} \qquad (6)$$

Combining the above reported Equations (6) it is possible to obtain the vehicle sideslip angle according to the Classic Kinematic Bicycle Model

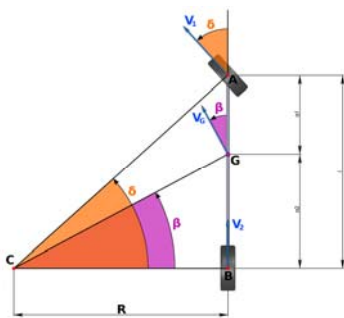$$\beta_0 = \tan^{-1}\left(\frac{a_2}{l}\cdot\tan\delta\right) \qquad (7)$$

Fig. 6. 'Classic' Kinematic Bicycle Model.

In the procedure (3B) the Classic Dynamic Bicycle model is used. Taking into consideration the presence of a certain sideslip angle makes the model closer to reality than the above kinematic model, since greater speeds and real manoeuvres can be considered.

Also in this case the input signals for this subsystem are the vehicle's longitudinal speed (u) and the steering angle of the vehicle's front wheels (δ).

Making use of these signals, the u and v quantities can be determined by means of the following Equations [16]:

$$\begin{Bmatrix}\dot{v}\\\dot{r}\end{Bmatrix} = -\begin{bmatrix}\dfrac{C_1+C_2}{u\cdot m} & \dfrac{C_1\cdot a_1 - C_2\cdot a_2}{u\cdot m}+u\\[2mm]\dfrac{C_1\cdot a_1 - C_2\cdot a_2}{J_z\cdot u} & \dfrac{C_1\cdot a_1^2 + C_2\cdot a_2^2}{J_z\cdot u}\end{bmatrix}\cdot\begin{Bmatrix}v\\r\end{Bmatrix}+C_1\cdot\delta\cdot\begin{Bmatrix}1/m\\a_1/J_z\end{Bmatrix} \quad (8)$$

After v and r have been determined, the vehicle's slip angle can be obtained (2).

VI. RESULTS AND CONCLUSION

The vehicle slip angle estimation method that exhibits the best fit with what is physically expected is obtained by procedures 1Cbis (GPS with differential correction), 3A and 3B (Bycicle Model) (Fig. 7). The other GPS based procedures still provide good results (Fig. 8). In revers, INS based methods show results not compliant with physical expectations probably due to errors in Euler Angles' estimation attributable to the magnetometer, whose signal is highly affected by the metallic masses on-board the test vehicle. Future analysis and experimental activities will provide a sounder base for the claim of the better performance of procedures 1Cbis, 3A and 3B. Future
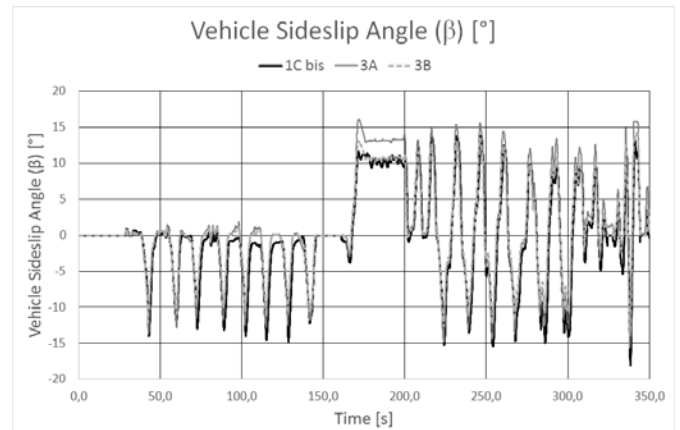

Fig. 7. Comparison between vehicle sideslip angle measured by GPS-based Differential Procedure (Procedure 1C bis), Kinematic Bicycle Model (Procedure 3A) and Dynamic Bicycle Model (Procedure 3B).
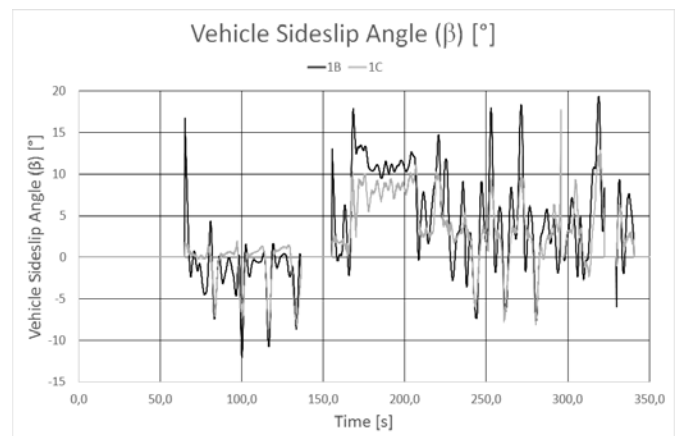

Fig. 8. Vehicle sideslip angle with Procedures 1B and 1C XSENS.

experiments will also be carried out according to a designed experimental plan, and results from the experimental campaign will be analyzed by means of statistical data analysis techniques to determine the influence of some relevant factors on the estimates provided by the different methods [22]-[26].

Future developments will also deal with a real-time GPS differential procedure, with a double antenna GPS procedure, with combined methods able to fuse signals coming out from different devices treating them by means of statistical methods.

REFERENCES

[1] R. Rajamani, "Vehicle Dynamics and Control", Springer, 2012.
[2] R. Russo, M. Terzo, F. Timpone, "Software in the loop development and validation of a Cornering Brake Control logic", *Vehicle System Dynamics*, vol. 45, pp. 149-163, 2007.
[3] M. Carro, M. Russo, F. Timpone, "A modern approach to design optimization and development of vehicles control systems", *Proceedings of the Mini Conference on Vehicle System Dynamics, Identification and Anomalies*, pp. 603-610, 2002.
[4] M. Terzo, F. Timpone, "The control of the handling of a front wheel drive vehicle by means of a magnetorheological differential", *International Review of Mechanical Engineering*, Volume 7, Issue 3, Pages 395-401, 2013.
[5] D. Piyabongkarn, R. Rajamani, J. A. Grogg, J. Y. Lew, "Development and Experimental Evaluation of a Slip Angle Estimator for Vehicle Stability Control", *IEEE transactions on control systems technology*, vol. 17, n. 1, 2009.
[6] G. N. Bifulco, L. Pariota, F. Simonelli, R. Di Pace, "Development and testing of a fully Adaptive Cruise Control system", *Transportation Research Part C: Emerging Technologies*, vol. 29, pp. 156-170, 2013.
[7] M. Doumiati, A. Victorino, D. Lechner, G. Baffet, A. Charara, "Observers for vehicle tyre/road forces estimations: experimental

validation", *Vehicle System Dynamics*, vol. 48, no. 11, pp. 1345-1378, 2010.

[8] X. Gao, Z. Yu, "Nonlinear Estimation of Vehicle Sideslip Angle Based on Adaptive Extended Kalman Filter", *SAE Technical Paper*, no. 2010-01-0117, 2010.

[9] F. Farroni, M. Russo, R. Russo, F. Timpone, "A physical–analytical model for a real-time local grip estimation of tyre rubber in sliding contact with road asperities", *Proceedings of the Institution of Mechanical Engineers, Part D: Journal of Automobile Engineering*, vol. 228, no. 8, 2014.

[10] H. F. Grip, L. Imsland, T. A. Johansen, T. I. Fossen, J. C. Kalkkuhl, A. Suiss, "Nonlinear vehicle side-slip estimation with friction adaption", *Automatica*, vol. 44, pp. 611-622, 2008.

[11] J. Ryu, E. J. Rossetter and J. C. Gerdes, "Vehicle Sideslip and Roll Parameter Estimation using GPS", *Proceedings of the AVEC International Symposium on Advanced Vehicle Control*, 2002.

[12] D. N. Piyabongkarn, R. Rajamani, J. A. Grogg, J. Y. Lew, "Development and Experimental Evaluation of a Slip Angle Estimator for Vehicle Stability Control," *IEEE Transactions On Control Systems Technology*, vol. 17, no. 1, 2009.

[13] G. J. Morgan-Owen, G. T. Johnston, "Differential GPS Positioning", *Electronics & Communication Engineering Journal*, vol. 7, no. 1, 1995.

[14] P. Misra and P. Enge, "Global Positioning System - Signals, Measurements and Performance", Lincoln (MA), Ganga-Jamuna Press, 2004.

[15] A. D. King; Marconi Electric Systems (MES), "Inertial Navigation - Forty Years of Evolution", *GEC (General Electric Company) Review*, vol. 13, no. 3, 1998.

[16] M. Guiggiani, "The Science of Vehicle Dynamics", Springer, 2014.

[17] F. Farroni, M. Russo, R. Russo, M. Terzo, F. Timpone, "A combined use of phase plane and handling diagram method to study the influence of tyre and vehicle characteristics on stability", *Vehicle System Dynamics*, vol. 51, pp. 1265-1285, 2013.

[18] A. Montella, L. Pariota, F. Galante, L. Imbriani, M. Mauriello, "Prediction of Drivers' Speed Behaviour on Rural Motorways Based on an Instrumented Vehicle Study", *Transportation Research Record: Journal of Transportation Research Board*, Transportation Research Board of the National Academies, Washington, D.C., n. 2434, pp. 52-62, 2014.

[19] G. N. Bifulco, L. Pariota, M. Brackstone, M. McDonald, "Driving behaviour models enabling the simulation of Advanced Driving Assistance Systems: revisiting the Action Point paradigm", *Transportation Research Part C: Emerging Technologies*, n. 36, pp. 352-366, 2013.

[20] F. Farroni, D. Giordano, M. Russo, M. Terzo, F. Timpone, "On the influence of anti-roll stiffness on vehicle stability and proposal of an innovative semi-active magnetorheological fluid anti-roll bar*", RAAD 2012 - 21TH International Workshop on Robotics in Alpe-Adria-Danube Region* - ISBN No: 978-88-95430-45-4.

[21] F. Farroni, "Development of a grip & thermodynamics sensitive tyre/road interaction forces characterization procedure employed in high-performance vehicles simulation", PhD thesis, University of Naples "Federico II", 2014.

[22] A. M. Lesk, "On the calculation of Euler angles from a rotation matrix", *International Journal of Mathematical Education in Science and Technology*, vol 17, no. 3, 1986.

[23] L. Angrisani, M. D'Apuzzo, D. Grillo, N. Pasquino, R. Schiano Lo Moriello, "A New Time-Domain Method for Frequency Measurement of Sinusoidal Signals in Critical Noise Conditions", *Measurement*, vol. 49, no. 1, pp. 368–381, 2014
doi: 10.1016/j.measurement.2013.11.034;

[24] P. Bifulco, A. Marrese, N. Pasquino, R. Schiano lo Moriello, "Statistical Characterization of Human Exposure to GSM Electromagnetic Field", *20th IMeKO TC4 Int. Symp.*, pp. 780-785, Benevento – Italy, July 15-17, 2014.

[25] P. Cennamo, P. Caputo, A. Giorgio, A. Moretti, N. Pasquino, "Biofilms on Tuff Stones at Historical Sites: Identification and Removal by Nonthermal Effects of Radiofrequencies", *Microbial Ecology*, vol. 66, no. 3, pp. 659-668, 2013.

[26] M. D'Arco, A. Liccardo, N. Pasquino, "ANOVA-Based Approach for DAC Diagnostics", *IEEE Trans. Instrum. Meas.*, vol. 61, no. 7, pp. 1874-1882, 2012.

[27] G. Betta, D. Capriglione, N. Pasquino, "Experimental Investigation on Workers' Exposure to Electromagnetic Fields in Proximity of Magnetic Resonance Imaging Systems", *Measurement*, vol. 45, no. 2, pp. 199-206, 2012.